Development and Testing of a 2-D Transfer CCD

David R. Smith, Andrew D. Holland, Adrian Martin, David Burt, Tim Eaton, and Roy Steward

***Abstract*—This paper describes the development, operation, and characterization of charge-coupled devices (CCDs) that feature an electrode structure that allows the transfer of charge both horizontally and vertically through the image area. Such devices have been termed two-dimensional (2-D) transfer CCDs (2DT CCDs), as opposed to the conventional devices, which might be called one-dimensional transfer CCDs, but in other respects are the same as conventional CCD devices. Batches of two different 2DT CCD test devices, featuring different electrode structures but with identical clocking operation in each case, were produced and tested. The methodology of 2-D charge transfer in each of the device types is described, followed by a presentation of test results from the new CCDs. The ability of both 2DT CCD transfer electrode schemes to successfully transfer charge in both horizontal and vertical directions in the image section of the devices has been proven, opening up potential new applications for 2DT CCD use.**

***Index Terms*—Charge-coupled device (CCD), charge injection, charge transfer, Gaia, radial velocity spectrometer (RVS), two-dimensional transfer CCD (2DT CCD).**

I. Introduction

An early application of two-dimensional (2-D) charge transfer in a charge-coupled device (CCD) was proposed by e2v technologies ltd. (then known as EEV) in 1990 for use as a scan converter. The electrode structure necessary for 2-D charge transfer was implemented in four poly-silicon levels. Such devices were subsequently proposed in 1992 as part of a European Space Agency study to develop a subpixel cloud monitor for a scanning radiometer earth observation instrument [1]. In conventional devices, image exposure can occur in synchronization with a moving image, in so-called time delay integration (TDI) mode. However, this method of operation only works for images moving parallel to the CCD columns. The use of 2-D transfer CCDs (2DT CCDs) allowed the CCD image to be shifted both horizontally and vertically during image integration to match the interframe drift, significantly reducing image smear and improving the cloud detection performance. Imaging 2-D transfer devices were also developed by researchers at Lincoln Laboratory, Massachusetts Institute of Technology, in 1994 [2], [3]. These so-called orthogonal-transfer CCDs have been tried in a number of applications for the purpose of compensating for any relative image motion between the CCD detector and the target, for example, in machine vision systems featuring moving objects [4] and in ground-based adaptive optics systems [5]–[7]. More recently, a 2DT CCD development program was initiated as part of the CCD development program for the radial velocity spectrometer (RVS) instrument of the European Space Agency's cornerstone Gaia mission [8]. The CCDs of the RVS instrument will operate in TDI mode, where the scan rate of the sky across the imaging area of a device is synchronized with the readout rate of the device, the spacecraft scan direction being aligned with the conventional parallel readout direction of the CCD. The lateral shift in the image varies sinusoidally over the spacecraft's 6-h scan period by up to ± 11 pixels across the CCD, thereby adding significant blurring to the recorded images. The 2DT CCD design allows for the orthogonal correction of the shifted charge patterns observed during readout of the RVS devices, providing the ability to track the moving charge without the need for any additional instrument mechanism.

This paper describes the testing of two different batches of 2DT CCDs that were developed as part of the Gaia RVS CCD program. Each batch featured devices with a specific electrode structure, the two different electrode structures allowing for the 2-D transfer of charge within the imaging region in each case. All the supplied CCDs also contained a charge injection structure at the top of the main imaging area of each device, enabling a quantity of charge to be injected into the central pixel of the top row of the image area. From this position, the injected charge could then be moved around the image array in both horizontal and vertical directions by the 2DT CCD electrode structure, allowing for a detailed assessment of the operational properties of the device, as presented below.

II. 2DT CCD

A. 2DT CCD Design

The two different electrode structures used by the 2DT CCDs, designated "Type 1" and "Type 3," are illustrated in Figs. 1 and 2, respectively. This designation results from the initial 2DT CCD paper design study that gave four electrode structure options, two of which were selected for progression to silicon manufacture. In each case, the presented schematic shows the top of the CCD imaging area, including the injection diode (ID) and injection gates (IG1 and IG2) of the charge injection structure, along with the bottom of the device featuring the transfer gates (TG) to the serial readout register, which are driven in common with $I\phi 3$. The number of pixels from the top of the device to the bottom of the device has been reduced to five pixels, from the full 1200 pixels, for ease of illustration.

Manuscript received May 16, 2006; revised August 22, 2006. The work of D. R. Smith was supported by the U.K. Particle Physics and Astronomy Research Council. The authors would like to thank e2v Technologies for supplying the 2DT CCD test devices and the Europian Space Agency for support and financing the program. The review of this paper was arranged by Editor J. Hynecek.

D. R. Smith and A. D. Holland are with the e2v Centre for Electronic Imaging, Brunel University, UB8 3PH Uxbridge, U.K. (e-mail: david.smith@brunel.ac.uk).

A. Martin was with the e2v Centre for Electronic Imaging, Brunel University, UB8 3PH Uxbridge, U.K. He is now with Sensor Sciences, LLC, Pleasant Hill, CA 94523 USA.

D. Burt, T. Eaton, and R. Steward are with e2v Technologies Ltd., CM1 2QU Essex, U.K.

Digital Object Identifier 10.1109/TED.2006.884072

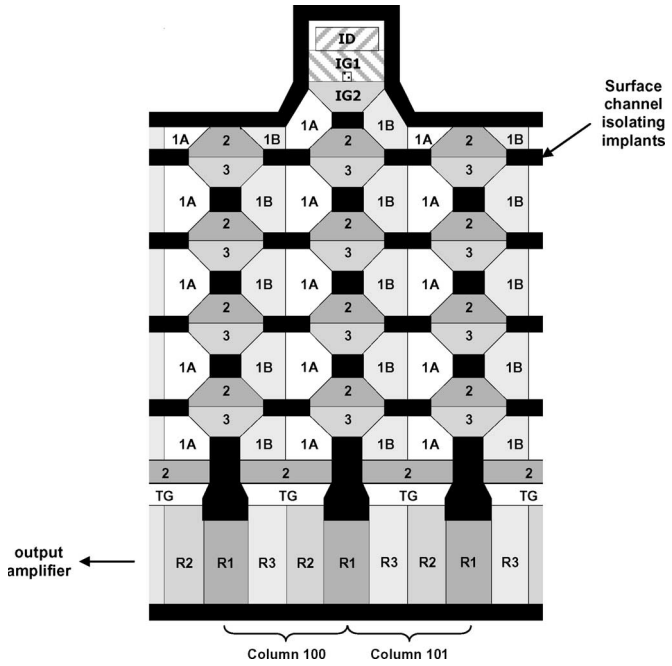

Fig. 1. Type 1 2DT CCD electrode structure.

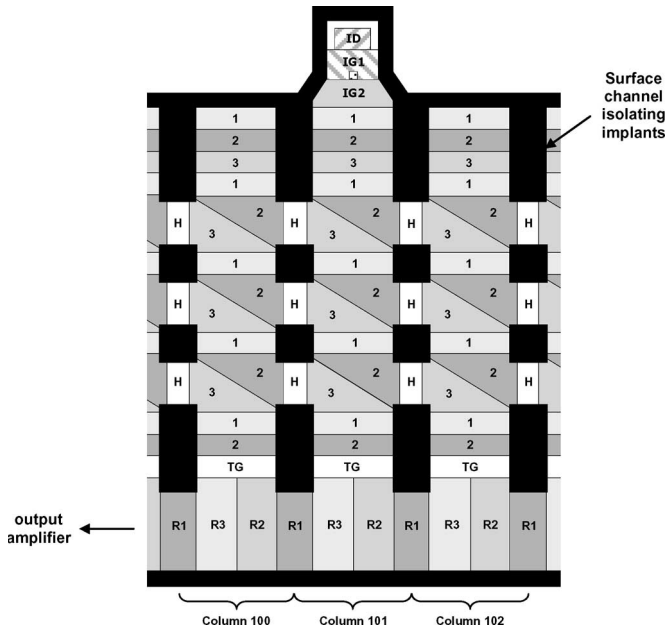

Fig. 2. Type 3 2DT CCD electrode structure.

The CCD column numbers, electrode numbering scheme (for the Type 3 devices, "H" is the "horizontal" transfer electrode), and serial register electrodes (R1, R2, and R3) are also labeled in the figures.

B. 2DT CCD Test Devices

Two batches of three 2DT CCD devices were provided for characterization: one batch featuring devices with the Type 1 electrode structure, and the other featuring devices with the Type 3 electrode structure. Both types of CCD were full-frame operation devices, each with 200 pixels × 1200 pixels of 15 μm × 10 μm and featuring a charge injection structure above the center of the first imaging row. The readout register of each device was a standard three-phase serial clocking register. The device characteristics are summarized in Table I. Fig. 3 shows a photograph of one of the 2DT CCD test devices, including a match head for scale comparison.

TABLE I
2DT CCD DEVICE CHARACTERISTICS

Parameter	Value
Device operation	Full frame
Image size	200 pixels × 1200 pixels
Pixel size	15 μm × 10 μm
Noise	~5 electrons r.m.s.
Full well capacity	~90k electrons

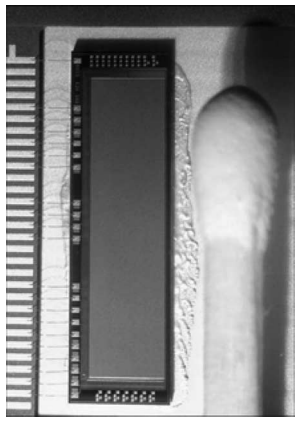

Fig. 3. Photograph of one of the 2DT CCD devices.

C. 2-D Charge Transfer

The necessary electrode structure in each 2DT CCD pixel to facilitate the lateral shifting of charge within the CCD imaging area is implemented in four separate poly-silicon layers. The methods of charge transfer in each of the two device types, for standard transfer down a column and for orthogonal transfer to the "left" and to the "right," are illustrated in Figs. 4 and 5 for the Type 1 and Type 3 devices, respectively. Each figure shows a six-pixel region of the given device and shows the flow of a charge packet in each CCD column during charge transfer.

The three different electrode clocking sequences used to move the charge down a column, to move the charge one column to the left, and to move the charge one column to the right were the same for both Type 1 and Type 3 devices. The actual sequence can be inferred from Figs. 4 and 5. The clocking pulses used in image transfer were of the order of 5-μs duration, the pulses overlapping by $\sim$1 μs to facilitate smooth charge transfer from under one electrode to the next without loosing a noticeable amount of charge into the trailing pixels. Further optimization of the clocking is possible and will be investigated in future device testing.

D. Charge Injection Operation

The charge injection structure at the top of each 2DT CCD was included to provide an electronic stimulation signal to

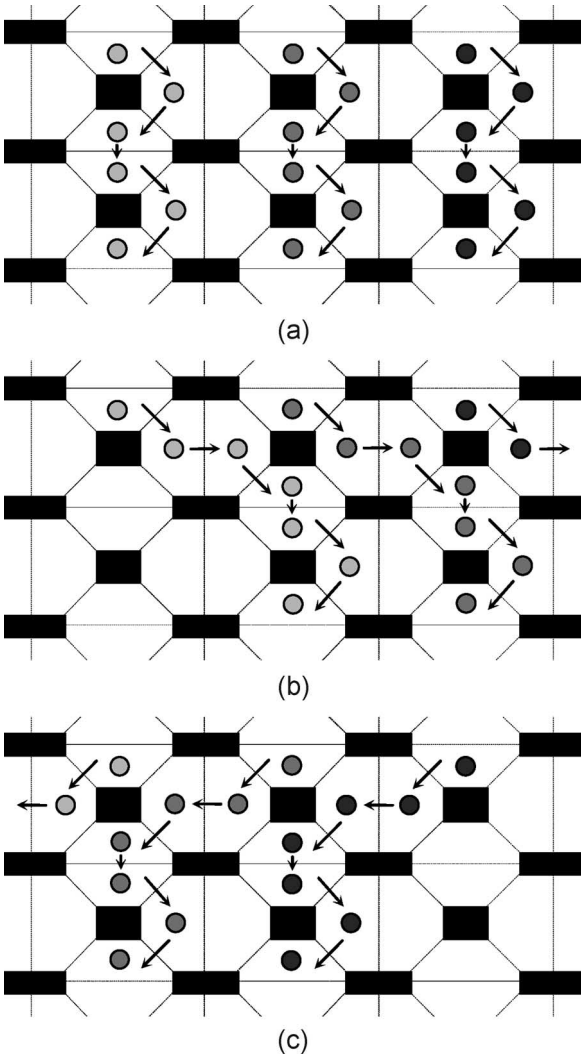

Fig. 4. Charge transfer in Type 1 2DT CCD. (a) Transfer down columns. (b) Transfer one column right and down. (c) Transfer one column left and down.

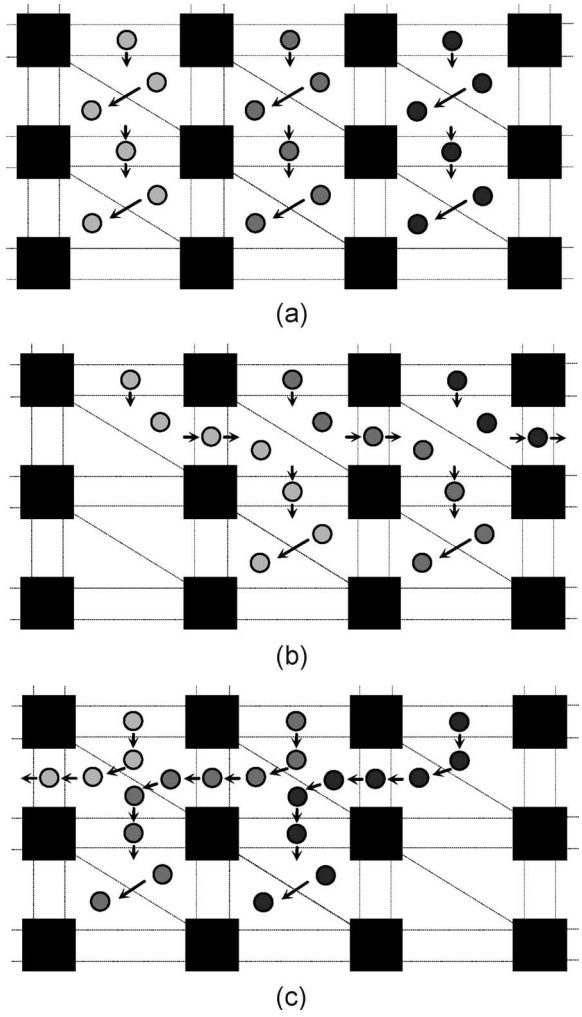

Fig. 5. Charge transfer in Type 3 2DT CCD. (a) Transfer down columns. (b) Transfer one column right and down. (c) Transfer one column left and down.

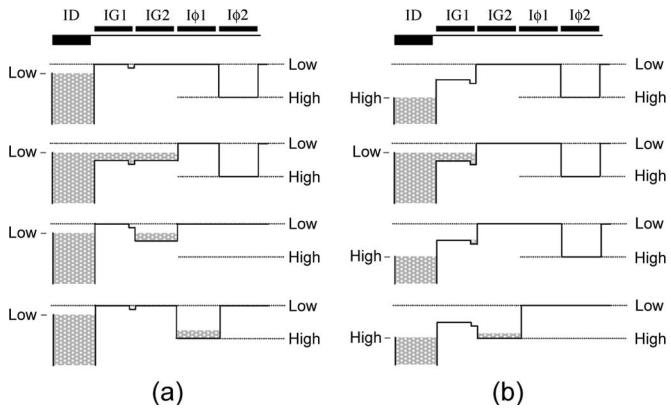

Fig. 6. Methods of charge injection in 2DT CCD devices. (a) Injection by pulsing IG1 and IG2. (b) Injection using the notched implant.

allow the characterization of the 2DT CCD operational properties. The injection structures in each 2DT CCD device type are illustrated in Figs. 1 and 2. Injection of charge into the center pixel of the first imaging row in each device (column 101 for both Type 1 and Type 3 devices) can be instigated by two methods. First, charge can be injected by pulsing the two injection gates IG1 and IG2, allowing charge to flow from the ID directly into the second injection gate IG2. From here, the charge can be clocked onto the first pixel in the column, as illustrated in Fig. 6. The injection structure of each CCD also features a small implant region under the first injection gate that creates a small supplementary potential well under IG1 adjacent to IG2, as illustrated in the device schematics in Figs. 1 and 2. By holding IG2 low, ID can be pulsed to allow charge to fill just the supplementary potential well, which can then in turn be passed onto IG2 when IG2 is made high. This second injection technique, also shown in Fig. 6, allows for the injection of small amounts of charge into the CCD array in a controllable manner. For the 2DT CCD characterization presented in this report, the first injection method described has been utilized, providing an injected signal level of $\sim$50 000 electrons. Fig. 7 shows the variation in charge injection signal with ID and IG for one of the Type 3 devices.

III. Device Characterization Methodology

Characterization of the 2DT CCD devices was performed using a vacuum chamber test facility incorporating a CryoTiger

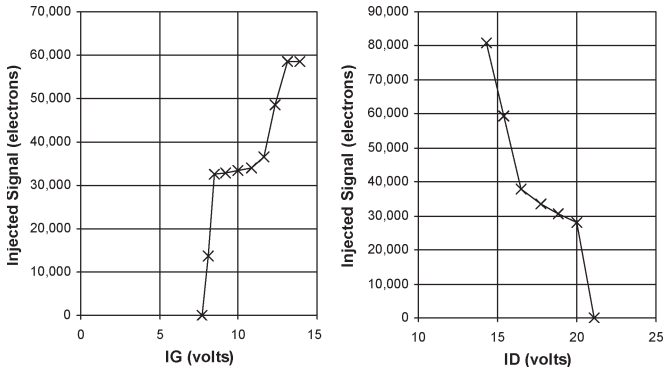

Fig. 7. Variation in the injected charge signal with ID and IG voltage for Type 3 2DT CCD.

TABLE II
OVERVIEW OF THE 2DT CCD TESTING

Test	Temperature (°C)
Functional test	20
Charge injection operation	20, -110
2D charge transfer operation	20, -110
Cosmetic quality	20, -110
Gain calibration	-110
Readout noise	-110
Leakage current	-50
Charge transfer efficiency	-110
Pixel charge capacity	-110

cooling system to enable testing from 0 °C to −130 °C. Each device was tested separately under vacuum, the CCD and preamplifier headboard being mounted onto a copper cold finger attached to the CryoTiger cold head within the test chamber. Temperature control was provided by use of a Lakeshore controller (model number 331) using a PT-1000 resistor mounted on the copper cold finger in close proximity to the CCD. The temperature of the CCD could be maintained to within ±0.05 °C at operating temperatures down to −110 °C. An ^{55}Fe source, emitting primarily Mn–Kα X-rays of energy 5898 eV, with an activity of ∼50 counts per second (in the CCD), was mounted within the test chamber to enable gain calibration of each CCD. The CCD clocking and the various control bias lines were provided using test electronics supplied by Xcam Ltd.

Characterization of each 2DT CCD was undertaken initially at room temperature to verify the operation and functionality of each device before a more detailed series of tests was carried out with each device operating at −110 °C. The lower temperature of −110 °C corresponds to the current baseline operational temperature for the RVS CCDs on Gaia, and it is at this temperature that a majority of the orthogonal clocking verification was performed. The various tests carried out on each device at the two different temperatures are described in the subsections below and are summarized in Table II.

A. Functional Test

After the initial switch on of a device at room temperature, the output from the CCD was fed into an oscilloscope for simple verification of device operation.

B. Charge Injection Operation

The operation of the charge injection structure was initially tested at room temperature to verify the ability of the structure to successfully inject charge into the imaging array of the CCD. The injection structure was then used in the charge transfer efficiency (CTE) and charge capacity testing at −110 °C as described below.

C. 2-D Charge Transfer Operation

The ability of each device to transfer charge horizontally, both to the "left" and "right," in the imaging area was tested at room temperature prior to a more detailed study of the CTE of the orthogonal clocking at −110 °C.

D. Cosmetic Quality

A number of full-frame CCD images were recorded at room temperature to observe any pixel or column defects that may have been present in the device.

E. Gain Calibration

Using the ^{55}Fe source as a reference energy, the gain of each device was derived in electronvolts per analog-to-digital converter (ADC) channel while operating at −110 °C.

F. Readout Noise

The background readout noise (including system noise) was taken to be the amount of charge observed in the overscan pixels measured in electrons per pixel at −110 °C.

G. Leakage Current

The additional nonsignal charge leakage current in each pixel was measured at −50 °C as electrons per pixel per second.

H. CTE

The CTE of orthogonal charge movement in the imaging array of each device was measured while operating at −110 °C using injected charge signal. To produce a measurable amount of charge loss between adjacent columns, the signal was injected into every eighth pixel in the central column of the device and then shifted five pixels left and five pixels right. This cycle was repeated 50 000 times, representing 500 000 left and right transfers. The pixels surrounding the central column were then analyzed for any sign of deferred charge from the original injection pixel.

I. Pixel Charge Capacity

To measure the charge capacity, or full well capacity, of the pixels in each 2DT CCD, increasing quantities of charge were

TABLE III
2DT CCD CLOCK AND BIAS VOLTAGES

Clock/Bias	Voltage (V)
Image clocks	6.7 (Type 1)*, 10.0 (Type 3)*
Clock 'low' voltage	0.0
Serial clocks	11.0*
Reset	9.3*
Injection diode	17.7
Output diode	27.9
Reset diode	20.3
Substrate	4.6

* these voltages are the upper limit used

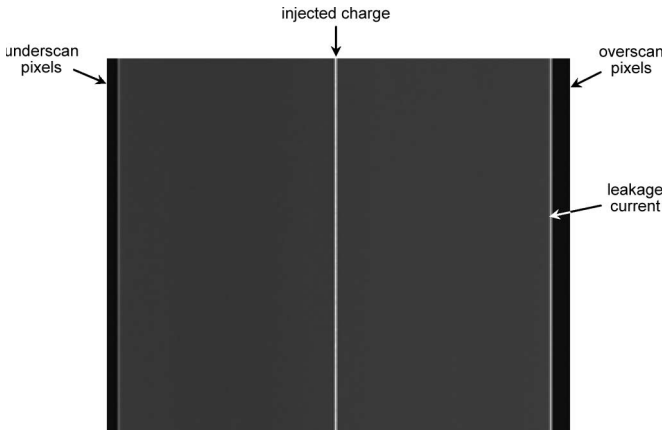

Fig. 8. CCD image taken at room temperature from Type 3 2DT CCD showing continuous charge injection into every row of the central column of the image area.

injected into single CCD pixels until the charge was observed to spill into adjacent pixels. The fraction of charge spilled from the injected pixel was then subtracted from the known injection level to obtain the full well capacity, measured to the nearest 500 electrons. The charge capacity measurements were recorded at -110 °C.

IV. ROOM TEMPERATURE CHARACTERIZATION

All six 2DT CCD devices were found to be functional during testing at room temperature. The quality of the CCD image area was very good in all six of the tested devices, with no bright or dark columns or pixels being evident at room temperature (or when subsequently operated at -110 °C) and uniform leakage current distribution. The three Type 1 CCDs did exhibit some slight streaking in the leakage current pattern along the columns of the device that could be removed with reduction of the image clock voltage from 10.0 to 6.7 V. All devices featured increased leakage current at the perimeter, producing bright edges to the recorded images. For the successful operation of both Type 1 and Type 3 devices, the clock voltages and biases listed in Table III were used. During characterization and testing of the CCDs, the readout speed was $\sim$75 kHz.

The injection structure was found to operate as designed in all devices. Fig. 8 shows a recorded CCD image from one of

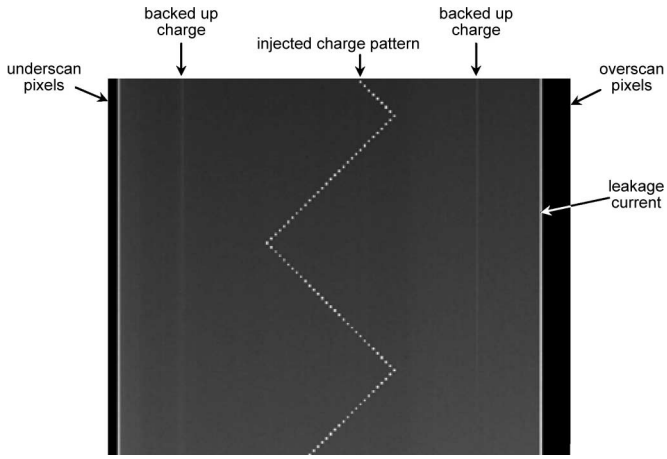

Fig. 9. CCD image taken at room temperature from Type 3 2DT CCD showing charge injection into every third row of the central column of the imaging area while horizontally shifting the image right and then left.

the Type 3 devices, charge injection into the central column of the device occurring in every row during readout. The injected charge, excess leakage current at the edges of the device, and underscan and overscan image regions can clearly be seen in the image.

The functionality of the orthogonal clocking sequence was also verified at room temperature. Fig. 9 shows a section of a recorded CCD image showing the injection pattern observed when injecting charge and transferring the image down three pixels and then right three pixels before injecting again. This is carried out 32 times before changing the lateral image movement to be three pixels to the left. Repeating this process builds up the "zig-zag" charge pattern seen in the figure. Charge was observed to build up at the edges of the CCD during horizontal transfer, where it cannot then escape from the periphery of the device, since in this implementation no dump register was included at the left and right edges of the CCD image area. This effect was reduced when operating at -110 °C, the amount of leakage current adding to the charge build up being reduced by the lower operating temperature. The charge build up at the edges of the device during orthogonal transfer is visible in the room temperature image shown in Fig. 9 and would need to be addressed in the full 2DT CCD design.

There is also some leakage current deposited into specific columns of the image array during orthogonal charge transfer, from the bright regions at each edge of the device. The two corresponding vertical bright streaks created are the same number of columns away from each edge of the device as the number of columns the image is shifted laterally and are clearly visible in the CCD image presented in Fig. 9. It should also be noted that the effective image size is reduced by the amount of lateral shift, any image area that is shifted beyond the edges of the CCD being lost.

The initial room temperature testing showed that both Type 1 and Type 3 2DT CCD devices operated as intended, all devices featuring fully functional charge injection structures and the ability to transfer charge laterally within the image area of each device.

TABLE IV
SUMMARY OF 2DT CCD TESTING RESULTS

Device Serial Number	Cosmetic Quality	System Gain (eV/channel)	Readout Noise (e^- r.m.s.)	Leakage Current (e^-/pixel/s at -50 °C)	Pixel Charge Capacity (e^-)
Type 1 devices					
04342.10.42	Good	18.7	5.25	-	79,000
04342.10.13	Some column streaking	19.6	5.29	4.7	78,000
04342.10.14	Good	18.5	5.20	-	78,000
Type 3 devices					
04342.10.25	Good	19.0	4.67	-	64,000
04342.10.28	Good	18.7	4.75	2.1	76,500
04342.10.30	Good	17.9	4.08	-	70,500

V. LOW-TEMPERATURE CHARACTERIZATION

Low-temperature characterization of each 2DT CCD was performed at -110 °C for the various tests described in Section III. The leakage current of each device was also measured, but at a temperature of -50 °C. The charge injection structure was used to provide the required signal charge for CTE and full well capacity characterization.

To measure the CTE of a given device, a charge signal of $\sim$50 000 electrons was injected into every eighth pixel in the central CCD column and then shifted five pixels left and five pixels right 50 000 times (i.e., 500 000 pixel transfers). The pixels surrounding the central column were then analyzed for signs of charge lost from the corresponding injected pixel, allowing the calculation of the charge transfer inefficiency (CTI) of the device, where

$$\text{CTI} = 1 - \text{CTE}. \tag{1}$$

In carrying out this test, no charge loss from any injected pixel was observed above the image background level. Taking a 2σ noise threshold of ten electrons, an upper limit of 4×10^{-10} can be placed on the CTI arising from deferred charge, given by

$$\text{CTI} = 2\sigma/(Q \times N) \tag{2}$$

where Q is the number of injected electrons, and N is the number of pixel transfers.

It should be noted that some deferred charge may be recaptured, the signal charge being transferred through the same group of pixels over and over again, artificially improving the CTI. If, however, the total CTI is considered to be composed of three components, namely 1) $\text{CTI}_{\text{design}}$, 2) $\text{CTI}_{\text{process}}$, and 3) $\text{CTI}_{\text{traps}}$, the fact that the calculated CTI value is so low and the tested devices were not radiation damaged implies that the CTI contribution by the first two components is quite small.

The measured cosmetic quality, gain, readout noise, leakage current, and pixel charge capacity of each 2DT CCD tested are shown in Table IV along with the corresponding device serial number. It should be noted that the Gaia RVS specification of a full well capacity of 50 000 electrons is comfortably achieved by all six tested devices. With the exception of one device that had some column streaking, all CCDs had very good cosmetic quality, exhibiting no bright or dark columns or pixels at room temperature or at -110 °C.

VI. CONCLUSION

All six 2DT CCD devices characterized in this paper were found to be fully functional, with both Type 1 and Type 3 electrode structures successfully allowing the orthogonal transfer of charge in the imaging section of each device. All the devices had no significant cosmetic defects and exhibited comparable device gain, readout noise, and full well capacity. The slight difference in readout noise between the two device types is most likely the result of wafer-to-wafer variation during manufacture.

An upper limit of 4×10^{-10} has been placed on the 2DT CCD orthogonal-transfer CTI at -110 °C. The low CTI demonstrates that the 2DT CCD devices would be suitable for narrow field adaptive optics applications, for image stabilization over long duration, and where processing power can be traded with the loss of some pixels around the edge of the CCD image area.

This paper has demonstrated that the orthogonal charge transfer technique can meet the requirement specification for application in the CCDs of Gaia RVS, both Type 1 and Type 3 devices being suitable. However, the transfer of charge orthogonally to the left in a Type 1 device requires fewer subpixel transfer steps than in the Type 3 device; this simpler transfer process making it the preferred device type of the two.

The 2DT CCDs of Type 1 electrode structure showed some charge streaking along the column direction, but this effect was removed when operating with a slightly reduced image clock voltage. No detailed analysis of the observed streaking was carried out during the study presented in this paper, and this will be addressed in future work.

A recommendation that dump registers be included at the left and right edges of future 2DT CCD devices was made following this paper to allow the removal of excess charge build up during lateral image shifting.

REFERENCES

[1] R. E. Cole and A. D. Holland, "Sub-pixel cloud monitor study (RAL Agreement 2566)—Final report," University of Leicester, Leicester, U.K., Project Rep. SC_SPCM/1/93, 1993.

[2] B. E. Burke, R. K. Reich, E. D. Savoye, and J. L. Tonry, "An orthogonal-transfer CCD imager," *IEEE Trans. Electron Devices*, vol. 41, no. 12, pp. 2482–2484, Dec. 1994.

[3] B. E. Burke and J. L. Tonry, "Recent developments with orthogonal-transfer CCDs," in *Proc. SPIE*, 1997, vol. 3019, pp. 233–240.
[4] G. Olson, "Image motion compensation with frame transfer CCDs," in *Proc. SPIE*, 2002, vol. 4567, pp. 153–160.
[5] J. A. Gregory, B. E. Burke, B. B. Kosicki, and R. K. Reich, "Developments in X-ray and astronomical CCD imagers," *Nucl. Instrum. Methods Phys. Res. A, Accel. Spectrom. Detect. Assoc. Equip.*, vol. A436, no. 1, pp. 1–8, Oct. 1999.
[6] D. E. Groom, "Recent progress on CCDs for astronomical imaging," in *Proc. SPIE*, 2000, vol. 4008, pp. 634–645.
[7] B. Burke, J. Tonry, M. Cooper, G. Luppino, G. Jacoby, R. Bredthauer, K. Boggs, M. Lesser, P. Onaka, D. Young, P. Doherty, and D. Craig, "The orthogonal-transfer array: A new CCD architecture for astronomy," in *Proc. SPIE*, 2004, vol. 5499, pp. 185–192.
[8] A. D. Holland, M. Cropper, D. Katz, I. B. Hutchinson, R. M. Ambrosi, T. Stevenson, D. R. Smith, D. Walton, D. Burt, P. Pool, D. Morris, and T. Paulsen, "CCDs for the radial velocity spectrometer on Gaia," in *Proc. SPIE*, 2004, vol. 5251, pp. 253–260.

David R. Smith was born in 1977. He received the M.Phys. degree (with Hons.) in physics with space science and systems from the University of Kent, Canterbury, Kent, U.K., in 2000, and the Ph.D. degree from the University of Leicester, Leicester, U.K., in 2004. His Ph.D. thesis was entitled "Radiation damage in charge-coupled devices."

He has continued to do research in the field of radiation damage effects in CCDs and is currently a Lecturer with the School of Engineering and Design, Brunel University, Uxbridge, U.K. He has published a number of papers on the effects of proton damage on CCD operation, in particular the generation and characteristics of bright pixels exhibiting "random telegraph signal" behavior, and the effects of radiation damage on the operational characteristics of electron-multiplication CCDs.

Dr. Smith is a member of the Institute of Physics and the International Society for Optical Engineers.

Andrew D. Holland received the B.Sc. degree (with Hons.) in physics from Durham University, Durham, U.K., in 1984, and the Ph.D. degree from the University of Leicester, Leicester, U.K., in 1990. His Ph.D. thesis was entitled "Radiation effects in CCD X-ray detectors."

He has 20 years of experience in the development of CCD and other imaging detectors and systems for science and industrial applications and is currently the Head of the Imaging for Space and Terrestrial Applications group with the School of Engineering and Design, Brunel University, Uxbridge, U.K. He has previously worked on a range of detector developments including XMM/EPIC and Swift.

Prof. Holland is a member of the International Society for Optical Engineers.

Adrian Martin received the B.Eng. degree in electrical and electronic engineering from City University, London, U.K., in 1991, the M.Sc. degree in spacecraft engineering from University College London, London, in 1995, and the Ph.D. degree from the University of Leicester, Leicester, U.K., in 2000. His Ph.D. thesis was entitled "Microchannel plate optics."

He was with the University of California, Berkeley, from 2000 to 2003, and the e2v Centre for Electronic Imaging, Brunel University, Uxbridge, U.K., from 2004 to 2005. He is currently with Sensor Sciences, LLC, Pleasant Hill, CA, where he designs and builds UV and gamma ray instruments for spaceflight and research.

David Burt, photograph and biography not available at the time of publication.

Tim Eaton, photograph and biography not available at the time of publication.

Roy Steward received the B.Sc. degree (with Hons.) in applied physics from the University of Brighton (formerly Brighton Polytechnic), Brighton, U.K., in 1970.

Since 1970, he has been with e2v Technologies Ltd., Essex, U.K., where he was the Department Manager for the manufacture of first- and second-generation image intensifiers, and was the Engineering Manager for the Electronics Division. He has also been involved in the design and manufacture of scientific CCDs. He has managed numerous high-value projects for Gomos on Envisat and SXI on the Goes series of satellites. He is currently the Project Manager for the supply of CCDs for Gaia.